HHS Public Access

Author manuscript

Dev Dyn. Author manuscript; available in PMC 2019 January 01.

Published in final edited form as:

Dev Dyn. 2018 January ; 247(1): 170–184. doi:10.1002/dvdy.24590.

Ventral neural patterning in the absence of a Shh activity gradient from the floorplate

Angelo Iulianella[1,*], **Daisuke Sakai**[2], **Hiroshi Kurosaka**[3], and **Paul A. Trainor**[4,5]

[1]Department of Medical Neuroscience, Faculty of Medicine, Dalhousie University, and Brain Repair Centre, Life Sciences Research Institute, 1348 Summer Street, Halifax, Nova Scotia, Canada B3H 4R2

[2]Doshisha University, Graduate School of Brain Science, HC301 1-3 Tataramiyakodani, Kyotanabe, Kyoto 610-0394, Japan

[3]Department of Orthodontics and Dentofacial Orthopedics, Graduate School of Dentistry, Osaka University, 1-8 Yamada-Oka, Suita, OSAKA 565-0871, Japan

[4]Stowers Institute For Medical Research, 1000 E 50th Street, Kansas City, MO, USA

[5]Department of Anatomy and Cell Biology, University of Kansas Medical Center, Kansas City, KS, USA

Abstract

BACKGROUND—Vertebrate spinal cord development requires Sonic Hedgehog (Shh) signaling from the floorplate and notochord, where it is thought to act in concentration dependent manner to pattern distinct cell identities along the ventral-to-dorsal axis. While *in vitro* experiments demonstrate naïve neural tissues are sensitive to small changes in Shh levels, genetic studies illustrate that some degree of ventral patterning can occur despite significant perturbations in Shh signaling. Consequently, the mechanistic relationship between Shh morphogen levels and acquisition of distinct cell identities remains unclear.

RESULTS—We addressed this using *Hedgehog acetyltransferase* (*Hhat*^{Creface}) and *Wiggable* mouse mutants. *Hhat* encodes a palmitoylase required for the secretion of Hedgehog proteins and formation of the Shh gradient. In its absence the spinal cord develops without floorplate cells and V3 interneurons. *Wiggable* is an allele of the Shh receptor Patched1 (*Ptch1*^{Wig}) that is unable to inhibit Shh signal transduction, resulting in expanded ventral progenitor domains. Surprisingly, *Hhat*$^{Creface/Creface}$; *Ptch1*$^{Wig/Wig}$ double mutants displayed fully restored ventral patterning despite an absence of Shh secretion from the floorplate.

CONCLUSIONS—The full range of neuronal progenitor types can be generated in the absence of a Shh gradient provided pathway repression is dampened, illustrating the complexity of morphogen dynamics in vertebrate patterning.

*Corresponding author: angelo.iulianella@dal.ca.

Author Contributions

Conceived experiments: AI. Performed experiments: AI, DS, HK. Analyzed the data: AI, PT, DS, HK. Wrote the paper: AI, PT, DS, HK.

Introduction

The prevailing view of morphogen signaling in the developing spinal cord stipulates that opposing concentration gradients of secreted molecules, namely Shh ventrally, and Wnts and BMPs dorsally, act in concert to specify distinct cell fates along the dorsal-ventral axis. The system appears to be finely-tuned, since as little as 1nM changes in morphogen concentration is sufficient to drive alternate cell fates in neural explants cultured *in vitro* (Ericson et al., 1997; Briscoe et al., 2000; Dessaud et al., 2007; Dessaud et al., 2008; Dessaud et al., 2010). However, the activation of Shh signaling effectors, namely Gli transcription factors, helps create a pattern of neural progenitor domains along the dorsal-ventral axis (Stamataki et al., 2005; Dessaud et al., 2008). There are three Gli proteins, which collectively act as the principal transcriptional effectors of the Hedgehog pathway (Jacob and Briscoe, 2003; Matise, 2013). Gli1 and Gli2 are considered transcriptional activators, whereas Gli3 functions primarily as a repressor. However, Gli2 can function as a repressor in the absence of Gli3, and conversely, Gli3 can act as an activator in the absence of Gli2. Gli2 and Gli3 need to be proteolytically processed to form a transcriptional repressor that blocks the action of Gli proteins in activating target genes (Ruiz i Altaba, 1998; Sasaki et al., 1999; Wang et al., 2000; Persson et al., 2002; Bai et al., 2004; Wang et al., 2007). Thus, the ratio of activator and repressor forms of Gli proteins can influence the extent and effect of Shh signaling within the embryonic spinal cord.

Smoothened (Smo) activity within a specialized cell structure called the primary cilium, mediates Gli processing and activity, which in turn activates target gene expression. However, another central regulator of Shh signaling is the Shh receptor Patched1 (Ptch1), which limits cellular responsiveness to Shh by inhibiting the activity of the co-receptor Smoothened (Smo) (Chen and Struhl, 1996; Marigo et al., 1996; Stone et al., 1996; Zhang et al., 2001; Taipale et al., 2002; Cohen et al., 2015). When Hedgehog proteins bind to Ptch1, Ptch1 becomes endocytosed, which diminishes its inhibitory influence on Smo, tipping the balance towards activator forms of Gli proteins (Incardona et al., 2002). Gli transcriptional activity itself appears to be graded, which then leads to strong transcriptional upregulation of several key target genes, including *FoxA2*, *Nkx2.2*, and *Olig2*, which specify floorplate, V3 interneuron, and motorneuron progenitor programs, respectively (Briscoe et al., 2000; Motoyama et al., 2003; Bai et al., 2004; Lei et al., 2004; Stamataki et al., 2005; Dessaud et al., 2007; Dessaud et al., 2008; Briscoe and Small, 2015). This mutually repressive transcription factor network refines dorsal-ventral domains of neural progenitor cells (Huangfu et al., 2003; Huangfu and Anderson, 2005).

Shh gradient sensing is mediated by the primary cilium (Eggenschwiler and Anderson, 2007; Murdoch and Copp, 2010; Pal and Mukhopadhyay, 2015; He et al., 2017), and its importance in Shh signal transduction has been demonstrated by the loss of the ciliary structural or motor proteins, which results in phenotypes similar to loss of function mutations in Shh pathway components (Huangfu et al., 2003; Huangfu and Anderson, 2006; Caspary et al., 2007; Cortellino et al., 2009; Larkins et al., 2011; Qin et al., 2011; Bangs and Anderson, 2016). Key components of the Shh signaling pathway, such as Smo, are enriched in cilia (Huangfu and Anderson, 2006; Drummond, 2012). The sequestration of Smo in cilia allows for the processing of Gli into activated forms, which leads to the transcriptional

activation of target genes, including Ptch1 (Liu et al., 2005). In response to Shh signaling, Ptch1 becomes localized to the base of cilia where it inhibits further Smo-dependent activation of the Gli effectors (Rohatgi et al., 2007). This limits the extent of Shh signaling, facilitating the fine-tuning (or stabilization) of cell fates within developing neural tissue (Ribes and Briscoe, 2009).

To further illustrate the complexity of the Shh signaling, genetic studies in the mouse have shown that some degree of neural patterning can proceed despite a significant loss of Shh pathway components. In *Shh*$^{-/-}$ mutants, although motor neurons fail to form, V0, V1 and other interneurons are present, but are abnormally positioned (Chiang et al., 1996). However, the ventral patterning defects in Shh mutants can largely be rescued in *Gli3/Shh* double mutant mouse embryos, with the notable exception of floorplate and V3 interneuron identity (Litingtung and Chiang, 2000; Oh et al., 2009). Furthermore, the combinatorial loss of *Ptch1* and *Gli2* and *Gli3* also results in fairly normal neural patterning, particular with respect to dorsal cell types (Motoyama et al., 2003). The fact that in both cases, full restoration of ventral patterning was not observed, suggests that Shh signaling is most critically required for the ventral-most regions of the developing neural tube. In addition, the loss of Shh expression in the floorplate of the embryonic spinal cord did not dramatically alter ventral neural patterning. It did however alter gliogenesis, suggesting an early critical window of exposure to highly levels of Shh levels in the notochord sets up ventral progenitor domains (Tian et al., 2005; Chamberlain et al., 2008; Yu et al., 2013). This idea is supported by *in vitro* experiments involving naïve neural tissues, which show that the activation of ventral progenitor programs are highly sensitive to small changes in Shh levels over short periods of time (Ericson et al., 1997; Dessaud et al., 2007; Dessaud et al., 2010). The prolonged exposure to Shh serves to maintain established progenitor programs and over time define progressively more dorsal fates (Dessaud et al., 2010). Altogether, both genetic and *in vitro* studies support the notion that there is flexibility and adaptability in the response to Shh levels during neural patterning.

Another way to view these genetic studies is that Shh morphogen dynamics relies on the ability of negative regulators to alter target cell responsiveness to Shh gradients over time (Dessaud et al., 2007; Dessaud et al., 2010). This in turn may help explain the dramatic scaling of morphogen systems that occur in vertebrates (Uygur et al., 2016), with different species displaying over a 3000-fold difference in body size, ranging from a recently discovered New Guinean frog that is less than 8mm long to a blue whale at 25 meters. Indeed, how the scaling of morphogen gradients during embryonic pattering is achieved is one of the most interesting unsolved questions in developmental biology. Recent advances in live imaging have revealed that neural progenitor domains are highly regulative, adapting to changes during the growth of the neural tube (Xiong et al., 2013). This is due at least in part to the emergence of reciprocal inhibitory transcription loops that dynamically define progenitor domain boundaries (Ribes and Briscoe, 2009; Briscoe and Small, 2015). The critical determinant of patterning then becomes a function of the change in responsiveness of target cells to a Shh gradient. This principal has recently been demonstrated by comparing the response to Shh levels in chicken vs. zebra finch embryonic neural tubes (Uygur et al., 2016). The zebra finch embryo is the smaller organism, and relative to chicken embryos is more sensitive to changes in Shh levels. Importantly, it achieves this scaling of the Shh

gradient principally by reducing the Gli2 and Gli3 repressor to activator ratio, thereby making zebra finch neural cells intrinsically more responsive to Shh signaling. Thus a more nuanced view of how morphogen dynamics regulate patterning in the developing nervous system is emerging, one which does not rely solely on the strict interpretation of a Shh gradient to determine discrete cell fate choices along the dorsal-ventral neural axis.

We therefore set out to test whether the vertebrate nervous system could be patterned without a Shh gradient. We previously described the Hedgehog acyltransferase gene (*Hhat*$^{Creface/Creface}$) insertional mouse mutant in which the Hedgehog gradient is effectively abrogated (Dennis et al., 2012). Hhat is required to palmitoylate the diffusible cleaved N-terminal Shh peptide, *Shh-Np*, which facilitates dispersion of the active Shh peptide from source cells, thereby creating a Shh morphogen gradient (Pepinsky et al., 1998; Chamoun et al., 2001; Zeng et al., 2001). More recently, we reported a novel *Ptch1* mouse mutant called *Wiggable* (*Ptch1*$^{Wiggable/Wiggable}$ or *Ptch1*$^{Wig/Wig}$) that results in increased Shh signaling during embryo development (Kurosaka et al., 2014; Kurosaka et al., 2015). Interestingly, compound mutation of both *Hhat*^{Creface} and *Ptch1*^{Wig} rescued the effects of excess Shh signaling in *Ptch1*^{Wig} mutants with respect to craniofacial morphogenesis and cranial nerve patterning (Kurosaka et al., 2014; Kurosaka et al., 2015). This suggests that the patterning effects of Shh can occur without a gradient, provided that repressors of the pathway, which are in part controlled Ptch1, are removed.

We tested this hypothesis during spinal cord development in *Ptch1*$^{Wig/Wig}$ and *Hhat*$^{Creface/Creface}$ mouse mutants. Neural patterning in the spinal cord is a well-characterized system for exploring the role of Shh morphogen gradient in progenitor fate specification. Shh secreted from floorplate cells act to pattern ventral cell fates in the developing neural tube. However, we discovered that *Hhat*$^{Creface/Creface}$ mutants, which lack long-range Shh signaling, floorplate formation and ventral spinal cord patterning, can be completely rescued by the *Ptch1*^{Wig} mutation. Surprisingly, *Hhat*$^{Creface/Creface}$; *Ptch1*$^{Wig/Wig}$ double mutants exhibit normal floorplate, V3 interneuron, motoneuron, and ventral interneuron specification despite an absence of Shh signaling from the floorplate. These findings highlight the complex role of Shh signaling in pattern formation and suggest that an absolute gradient mechanism is not essential for the full elaboration of cell specification in the developing vertebrate neural tube.

Results

Ptch1^{Wig} mutants display enhanced Shh signaling response in the developing neural tube

The development of the neural tube is a classic model of pattern formation in response to graded morphogen signaling. Graded Shh signaling initially from the notochord, and then from the floorplate acts to specify ventral neural tube character in a dose and time-dependent manner (Briscoe and Small, 2015). Here we tested the requirement for the Shh activity gradient in ventral neural patterning using a genetic approach to alter the levels of Shh signaling during development. This was accomplished using *Ptch1*$^{Wig/Wig}$ and *Hhat*$^{Creface/Creface}$ mouse mutants. The *Ptch1*$^{Wig/Wig}$ mouse mutant originated from an ENU screen for craniofacial patterning defects, and produces a stable C-terminal truncated Patched1 protein (Sandell et al., 2011; Kurosaka et al., 2014; Kurosaka et al., 2015).

Hhat$^{Creface/Creface}$ mutant mice were generated as a result of *Cre* transgene insertion into the *Hhat* locus generating a null allele. Hhat is required to palmitoylate the cleaved cholesterol-modified form of Shh, allowing for secretion and long range Shh signaling (Pepinsky et al., 1998; Chamoun et al., 2001; Dennis et al., 2012).

We first examined whether the *Ptch1*^{Wig} mutation increased Shh signaling in the developing neural tube, by crossing *Ptch1*$^{Wig/+}$ mice to *Ptch1*$^{LacZ/+}$ mice. The *Ptch1*^{LacZ} allele is a complete loss of function allele in which *Ptch1* coding sequence was replaced with the *LacZ* gene (Goodrich et al., 1997; Motoyama et al., 2003). Ptch1 is both a receptor for Shh signaling and readout of Shh activity because it functions as a direct downstream target of Gli transcription factors (Taipale et al., 2002; Agren et al., 2004). E9.5 *Ptch1*$^{LacZ/+}$ embryos develop normally and Shh signaling (as β-galactosidase staining), is restricted to the ventral most region of the neural tube, notochord and surrounding mesenchyme (Fig. 1A, a′, a″). In contrast, *Ptch1*$^{Wig/LacZ}$ mutant embryos exhibit open neural tube defects similar to *Ptch1*$^{/Wig/Wig}$ embryos and display considerably increased β-galactosidase activity, indicative of enhanced Shh responsiveness throughout the neural tube (Fig. 1B, b′, b″). This is consistent with the failure of *Ptch*^{Wig} and *Ptch1*^{LacZ} to complement.

Ptch1^{Wig} mutants display expanded ventral neural patterning

The *Ptch1*^{Wig} mutation results in sustained Shh signaling activation, and we hypothesized this would disrupt ventral neural patterning in *Ptch1*$^{Wig/Wig}$ embryos. We used Nkx2.2 antibodies to label V3 interneuron progenitors, which are the ventral-most neuron class, FoxA2 to identify floorplate (FP) cells, Isl1 and Olig2 to label nascent motor neurons (MNs) and their progenitors (pMN), and Chx10 and Nkx2.2 to delineate the relationship between V2 and V3 interneurons. At E9.5, when ventral progenitor domains have been established in the spinal cord, *Ptch1*$^{Wig/Wig}$ mutants exhibited an expansion of FoxA2+ FP cells and Nkx2.2-labeled V3 interneurons (p3), and a slight dorsal shift of Olig2-expressing pMN (Fig. 2A-a‴, B-b‴). While the FP, V3, pMN were specified, boundaries were less distinct and there was a greater degree of co-expression of FoxA2 and Nkx2.2 in the *Ptch1*$^{Wig/Wig}$ mutants, suggesting excessive activation of the ventral-most progenitor cell types. Quantification of cell numbers revealed a 1.8–2-fold increase in FoxA2 and Nkx2.2 expressing cells in the E9.5 *Ptch1*$^{Wig/Wig}$ mutant spinal cord (Fig. 2C, $P<0.0001$, wild type N=3, mutant N=5). By E10.5, *Ptch1*$^{Wig/Wig}$ mutants displayed more severe dorsal shifts and expansions in the p3 and pMN domains relative to controls (Fig. 2D–G). The increased separation between V3 and V2 classes of interneurons coincided with an expanded domain of Olig2+ MN progenitors (Fig. 2F–G).

Similar to the *Ptch1*^{Wig} mutation, the *Ptch1*^{LacZ} null allele also sensitizes the embryonic nervous system to Shh signaling (Fig. 1). We therefore compared ventral spinal cord patterning in E10.5 *Ptch1*$^{Wig/Wig}$ and *Ptch1*$^{LacZ/Wig}$ mutants. Both mutants displayed a similar expansion of floorplate (*, Fig. 3A–C), p3 (*, Fig. 3D–F), and pMN (Fig. 3G–I) domains relative to controls, demarcated by the expression of Foxa2, Nkx2.2 and Olig2, respectively. Both mutants exhibited dorsal specification, as revealed by Pax6 immunostaining (Fig. 3J–L), however the domain was reduced compared to wild-type controls and contrasts with a previous report of a total absence of dorsal character in

Ptch1$^{LacZ/LacZ}$ null mutants (Goodrich et al., 1997). Thus, *Ptch1*$^{Wig/Wig}$ mutants display the same diversity of ventral progenitor types as found in wild type littermates, but the domains are expanded and shifted dorsally in the embryonic spinal cord. This phenotype contrasts with the *Ptch1*$^{LacZ/LacZ}$ null mutants, which show extensive ventralization of neural character via massive dorsal expansion of FoxA2 staining throughout the neural tube (Goodrich et al., 1997; Motoyama et al., 2003). Moreover, the *Ptch1*$^{LacZ/Wig}$ and *Ptch1*$^{Wig/Wig}$ mutants are viable until E11.5 unlike *Ptch1*$^{LacZ/LacZ}$ mutants, which are lethal at E9.5.

Ptch1^{Wig} fails to localize to cilia resulting in decreased Gli3 Repressor synthesis

Ptch1 is a downstream transcriptional target of Shh signaling that negatively regulates the pathway via repression of Smo in the primary cilium in vertebrate cells (Rohatgi et al., 2007). Given that *Ptch1*$^{/Wig/LacZ}$ mutants exhibit enhanced Shh activity as evidenced by increased LacZ activity from the Ptch1 locus (Fig. 1), we tested whether Ptch1^{Wig} protein could localize to the cilia upon Smo activation. We transfected the canine kidney cell line (MDCK II) with either myc-tagged full length Ptch1 or flag-tagged Ptch1^{Wig} expression constructs. We then stimulated Smo with 20-hydroxycholesterol and examined the localization of myc-Ptch1 or Flag-Ptch1^{Wig} using acetylated-α-tubulin as a marker of the primary cilium. As expected, full length Flg-Ptch1 localized to cilium in cultured cells (Fig. 4A–C). In contrast Flag-Ptch1^{Wig} failed to localize to the cilium and instead was highly dispersed throughout the cytoplasm and/or cell surface (Fig. 4D–F). We next examined the effect of *Ptch1*^{Wig} on the formation of Gli3 repressor in Western blots of lysates from mouse embryos by comparing the full length 190kDa activator form to the 83kDa repressor form, as described previously (Wang et al., 2007). *Ptch1*^{Wig} mutants showed a 2.3 fold increase in the 190/83kDa (activator/repressor) ratio relative to wild type littermate controls (0.80/0.35, $P = 0.017$, Student's t-test). This was indicative of a significant reduction in Gli3 repressor synthesis (Fig. 4G, H). Taken together, these data showed that Ptch1^{Wig} is unable to localize to the primary cilium following Smo activation, which results in reduced formation of a principal repressor of the Shh pathway, and consequently upregulation of Shh signaling.

Complete rescue of ventral patterning in Hhat$^{Creface/Creface}$; Ptch1$^{Wig/Wig}$ mutants

The morphogen gradient hypothesis states that cell fate is determined via a transcriptional response to differing levels of a morphogen. However, we hypothesized that proper dorsoventral patterning of the spinal cord might still be able to occur in the absence of a Shh gradient if downstream repressors of the pathway were also inhibited. Therefore we crossed the *Hhat*$^{Creface/Creface}$ allele into the background of *Ptch1*$^{Wig/Wig}$ mutants. Hhat is required for post-translational palmitoylation of Hedgehog (Hh) proteins, and in the absence of Hhat, Hh secretion from producing cells is diminished, which perturbs long-range Hh signaling. We used Pax6 and Shh immunostaining to reveal ventral interneuron progenitors and the sources of Shh respectively, in the developing spinal cord. In E10.5 wild type embryos, Pax6 labels a broad domain of ventral interneuron progenitors, while Shh protein is found in the floorplate and notochord (Fig. 5A). *Ptch1*$^{Wig/Wig}$ mutants displayed a dorsally shifted Pax6 domain and slightly expanded floorplate-secreting Shh (Fig. 5B), which is consistent with a Shh gain-of-function mutation (Fig. 4). In contrast *Hhat* $^{Creface/Creface}$ mutants lacked a floorplate as both Shh and Foxa2 were absent from the most ventral cells in the neural tube.

Shh was however detected in the notochord (Fig. 5C). *Hhat* $^{Creface/Crefac}$ mutants also displayed a striking reduction and near absence of Pax6-positive progenitors (Fig. 5C). Surprisingly, in *Hhat*$^{Creface/Creface}$; *Ptch1*$^{Wig/Wig}$ double mutants, despite an absence of Shh from the ventral most cells in the neural tube, the position of the Pax6-positive interneuron progenitor domain was restored (Fig. 5D).

Using FoxA2 to identify floorplate cells, we confirmed that *Ptch1*$^{Wig/Wig}$ mutants presented with an expanded floorplate (Fig. 5E vs. 5F), while *Hhat* $^{Creface/Creface}$ mutants lacked floorplate development altogether (Fig. 5G). *Hhat*$^{Creface/Creface}$; *Ptch1*$^{Wig/Wig}$ double mutants however exhibit floorplate development that is comparable to wild type littermates (Fig. 5E vs. 5H). Similarly, with respect to p3 development, we observed an expanded Nkx2.2 labeled p3 domain in *Ptch1*$^{Wig/Wig}$ mutants (Fig. 5I vs. 5J), and near complete p3 abolishment in *Hhat* $^{Creface/Creface}$ mutants (Fig. 5K), which is consistent with the respective increase or decrease in Shh signaling in those mutants. Surprisingly, the Nkx2.2-positve p3 domain was restored to normal in *Hhat*$^{Creface/Creface}$; *Ptch1*$^{Wig/Wig}$ double mutants (Fig. 5L). These findings demonstrate that ventral spinal cord neural patterning can occur essentially normally in the absence of Shh signaling from the floorplate, provided that downstream repression of the Shh pathway is reduced.

To further substantiate the absence of floorplate formation and identity in *Hhat*$^{Creface/Creface}$; *Ptch1*$^{Wig/Wig}$ mutants, we performed *Shh* in situ hybridization in E9.5 and E10.5 embryos. *Shh* mRNA is transcribed in the notochord and floorplate cells and provides an accurate read out of the acquisition of floorplate identity. At E9.5, *Shh* mRNA is transcribed in notochord and in the presumptive floorplate cells at the base of the neural tube (Fig. 6A). By E10.5, the floorplate acquires its characteristic flattened appearance and expresses high levels of *Shh* mRNA (Fig. 6E). *Ptch1*$^{Wig/Wig}$ mutants showed strong *Shh* transcription in the notochord and developing floorplate at E9.5 and E10.5 (Fig. 6B, * in 6F). In contrast *Hhat*$^{Creface/Creface}$ mutants displayed strong *Shh* expression in the notochord, and very limited expression if any in the presumptive floorplate at E9.5 (Fig. 6C). By E10.5, *Shh* expression was absent from the ventral hinge region of the neural tube in *Hhat*$^{Creface/Creface}$ (Fig. 6G). This region also lacked the flattened pseudostratified epithelial morphology of the floorplate (Fig. 6G). Interestingly, E9.5 and E10.5 *Hhat*$^{Creface/Creface}$; *Ptch1*$^{Wig/Wig}$ mutants exhibited high levels of *Shh* mRNA expression in both the notochord and developing floorplate (Fig. 6D, H). Moreover, the floorplate developed largely normally in these mutants, having a flattened pseudostratified appearance (Fig. 6H). We conclude that floorplate specification occurred normally in *Hhat*$^{Creface/Creface}$; *Ptch1*$^{Wig/Wig}$ mutants, despite the absence of long range (or graded) Shh signaling from the floorplate.

Notochordal Shh relays full patterning information to the ventral neural tube in Ptch1$^{Wig/Wig}$ mutants

Both the notochord and floorplate influence neural patterning through the activity of Shh signaling (Yamada et al., 1991; Echelard et al., 1993; Yamada et al., 1993; Ericson et al., 1995; Chamberlain et al., 2008). In E8.5 wild-type embryos, the notochord is closely juxtaposed to the neural tube, as can be visualized morphologically and via Shh localization (Fig. 7A). *Ptch1*$^{Wig/Wig}$ mutants displayed expanded Shh signaling activity in the notochord

and floorplate (*, Fig. 7B), while *Hhat*$^{Creface/Creface}$ mutants lack Shh in the ventral neural tube but maintain it in the notochord (Fig. 7C). Similarly, *Hhat*$^{Creface/Creface}$*; Ptch1*$^{Wig/Wig}$ double mutants also lack Shh activity in the ventral neural tube, but retain activity in the notochord (Fig. 7D). Therefore we hypothesized that the complete rescue of ventral neural pattering in *Hhat*$^{Creface/Creface}$*; Ptch1*$^{Wig/Wig}$ mutant embryos was likely due to contact or proximity of the notochord and ventral tube during early embryogenesis.

Consistent with the expanded Shh staining, we observed a greatly expanded FoxA2-positive floorplate domain in *Ptch1*$^{Wig/Wig}$ mutants relative to controls (*, Fig. 7E, F). In contrast, *Hhat*$^{Creface/Creface}$ embryos showed a considerably reduced FoxA2 domain (Fig. 7G). Interestingly, *Hhat*$^{Creface/Creface}$*; Ptch1*$^{Wig/Wig}$ double mutants displayed an intermediate phenotype relative to each single mutant, with a slightly expanded FoxA2-positive floorplate (Fig, 7H). A similar pattern was observed for the p3 domain, which was labeled by Nkx2.2 expression. In *Ptch1*$^{Wig/Wig}$ mutants, the domain of Nkx2.2 is greatly expanded (*, Fig. 7I, J), which in contrast was almost abrogated in *Hhat*$^{Creface/Creface}$ mutants (Fig. 7K). However, the p3 progenitor domain was largely restored to normal in *Hhat*$^{Creface/Creface}$*; Ptch1*$^{Wig/Wig}$ double mutants (Fig. 7L). These findings suggest that in the absence of Shh signaling from the floorplate, Shh signaling emanating from the notochord, in combination with reduced downstream repression of the pathway is sufficient to restore normal ventral patterning in *Hhat*$^{Creface/Creface}$*; Ptch1*$^{Wig/Wig}$ double mutant embryos. This is consistent with genetic studies in the mouse demonstrating a critical requirement of Shh in the notochord to initiate ventral patterning (Tian et al., 2005; Chamberlain et al., 2008; Yu et al., 2013).

To further test the ability of notochordal Shh to drive ventral pattering in the developing spinal cord, we generated *Shh*$^{-/-}$*; Ptch1*$^{Wig/Wig}$ double mutants. We co-stained neural tubes with Pax6 and Shh to illlustrate the relationship between ventral interneuron progenitors and Shh expressing tissues (floorplate and notochord) (Fig. 8A). *Ptch1*$^{Wig/Wig}$ displayed a wider gap between the Pax6-posititve progenitor domain and Shh-expressing floorplate relative to controls (Fig. 8B). *Shh*$^{-/-}$ mutants displayed Pax6 staining throughout the entire neural tube (Fig. 8C), consistent with previous reports (Echelard et al., 1993). Similar to *Hhat*$^{Creface/Creface}$ mutants (Fig. 5C), *Shh*$^{-/-}$ mutants lacked formation of a floorplate with its characteristic pseudostratified epithelial structure at the ventral base of the neural tube. *Shh*$^{-/-}$*; Ptch1*$^{Wig/Wig}$ double mutants also lacked a floorplate and furthermore displayed an expanded domain of Pax6-positve progenitors within the neural tube (Fig. 8D). This suggested that the *Shh*$^{-/-}$*; Ptch1*$^{Wig/Wig}$ mutants lacked proper ventral specification. Consistent with this idea, we characterized the development of p3 progenitors via Nkx2.2 staining. In *Ptch1*$^{Wig/Wig}$ mutants the domain of Nkx2.2 labeled p3 progenitors was expanded dorsally (*, Fig. 8E, F). In contrast, p3 progenitors were completely abrogated in *Shh*$^{-/-}$ single mutants (Fig. 8G) and in *Shh*$^{-/-}$*; Ptch1*$^{Wig/Wig}$ double mutants (Fig. 8H), illustrating the requirement for notochordal Shh signaling for ventral neural specification in the spinal cord.

Lastly, we also examined the requirement for notochord derived Shh in the formation of dorsal and medial interneurons using Pax3 and Pax2 co-staining. *Ptch1*$^{Wig/Wig}$ mutants displayed a diminished and dorsally contracted domain of Pax3 progenitors and Pax2-labeled medial interneurons (Fig. 8J vs. 8I). In contrast, both Pax3 and Pax2 territories were

expanded ventrally in *Shh*$^{-/-}$ mutants (Fig. 8L), which is consistent with a loss of Shh signaling and dorsalization of the spinal cord patterning. However, in *Shh*$^{-/-}$; *Ptch1*$^{Wig/Wig}$ double mutants, the Pax3 domain was partially restored to its dorsally restricted domain, while Pax2-labeled medial interneurons remained scattered throughout the ventral region of the neural tube (Fig. 8M). Thus, there was a partial restoration of dorsal-ventral patterning in *Shh*$^{-/-}$; *Ptch1*$^{Wig/Wig}$ double mutant embryos (Fig. 8M vs. 8I), with the notable lack of specification of the ventral-most cell types of floorplate and p3 progenitors.

When compared to the pattern of neuronal specification in *Hhat*$^{Creface/Creface}$; *Ptch1*$^{Wig/Wig}$ double mutants, these results illustrate the importance of Shh signaling from the notochord for proper dorsal-ventral specification of the spinal cord. Importantly, proper dorsal-ventral patterning can occur in the absence of Shh signaling from the floorplate if downstream inhibitors of the pathway such as Ptch1 are also reduced. However, inhibition of Ptch1 function is insufficient to restore proper dorsal-ventral patterning in neural tubes that lack Shh in both the floorplate and notochord.

Discussion

The morphogen hypothesis states that graded levels of Shh are required to establish the full range of progenitor cell fates in the ventral vertebrate neural tube (Ericson et al., 1997; Briscoe et al., 2000; Dessaud et al., 2007; Ribes and Briscoe, 2009; Briscoe and Small, 2015). The cell types closest to the source of Shh develop in response to the highest concentration of the morphogen, with tissues farther away being influenced by progressively lower levels. How subtle changes in the levels of a signaling factor, or duration of exposure, are converted to discrete domains of gene expression and specific cell types remains an area of active investigation. An emerging view suggests that short exposures to Shh morphogen activity are required to initiate gene activation programs that specify the ventral-most cell types of the nervous system (Tian et al., 2005; Dessaud et al., 2007; Chamberlain et al., 2008; Dessaud et al., 2010). Continued Shh signaling then acts to stabilize these ventral domains as well as establish more dorsal progenitor domains and promote gliogenesis in the ventral spinal cord (Dessaud et al., 2010; Yu et al., 2013). Yet it is clear from studies in both invertebrates and vertebrates that ligand concentrations alone are insufficient to evoke the subtle differences in gene expression networks that correlate with the acquisition of distinct cell fates. Here we provide genetic evidence that the full range of progenitor cell types in the ventral neural tube can arise in the absence of a Shh gradient, provided that the downstream repression of the pathway is also dampened.

In classical experimental systems used to interrogate morphogen signaling, including the fly larval wing imaginal disk and vertebrate neural tube, it has been shown that the response to Hh depends upon the length of time progenitor tissues are exposed to Hh signaling to fully engage a patterned response (Dessaud et al., 2007; Nahmad and Stathopoulos, 2009). However, there are fundamental differences in the gradient mechanism in invertebrates vs. vertebrates. In invertebrates, the free flow or diffusion of biomolecules from a source in a syncytial cytoplasm can readily establish a morphogen gradient (Briscoe and Small, 2015). In contrast, in the vertebrate nervous system, a dynamically growing pseudostratified neuroepithelium makes gradient establishment through diffusion of secreted molecules

difficult. Further complicating this issue is that Shh is a lipid modified secreted molecule adhering to cell membranes, and live imaging studies have shown that it can be carried on cytoplasmic extensions of source cells called cytonemes to influence fate several cell diameters away (McMahon and Hasso, 2013; Sanders et al., 2013; Xiong et al., 2013). These findings suggest that Shh may not work as a traditional morphogen gradient producing specific cell fate responses according to a strict interpretation of the ligand concentration. Furthermore, *in vitro* explant experiments show that the length of time uncommitted neural tissue is exposed to Shh has as profound an effect on their differentiation as does concentration (Dessaud et al., 2007). This phenomenon is called 'temporal adaptation' and demonstrates the highly dynamic nature of Shh signaling during neural development.

Novel mouse models for the interrogation of morphogen gradient dynamics in neural patterning

A key component of the temporal adaptation mechanism is negative feedback control of the Shh signaling pathway. This is governed by the Shh receptor Ptch1, which is also a Shh target gene (Agren et al., 2004). Thus, after Shh activation, continued activation in target tissues is quickly dampened by upregulating the Shh inhibitor, Ptch1 (Cohen et al., 2015). Sustained pathway activity would therefore require continually increasing the levels of Shh signaling to overcome the reciprocal increase in Ptch1-mediated inhibition. Abrogating Ptch1 however, would de-couple this inhibitory feedback and lead to increased sensitivity of target cells to changes in Shh signaling levels.

The *Ptch1*^{Wig} mutation was generated in an ENU screen and comprises a point mutation in *Ptch1* that leads to a premature truncation after amino acid 878 (Kurosaka et al., 2015). *Ptch1*$^{Wig/Wig}$ mutant embryos show increased Shh signaling in the neural tube, which is consistent with our previous observations of elevated Shh signaling in the developing craniofacial complex (Kurosaka et al., 2014) and cranial ganglia (Kurosaka et al., 2015). Intriguingly, the *Ptch1*$^{Wig/Wig}$ mutant phenotype is not as severe as the *Ptch1*$^{LacZ/LacZ}$ phenotype. *Ptch1*$^{Wig/Wig}$ mutants are lethal at E11.5 and display the full range of progenitor identities in the developing neural tube, despite the expansion of all ventral cell types, including floorplate, p3, and pMN domains. In contrast, *Ptch1*$^{LacZ/LacZ}$ embryos are lethal at E9.5 and display extensively ventralized neural tube patterning together with loss of most dorsal cell types (Goodrich et al., 1997; Motoyama et al., 2003). One explanation for the differences in severity and phenotype between the two *Ptch1* alleles is that the *Ptch1*^{Wig} allele still retains some functionality with respect to regulating Shh signal transduction. In support of this idea, *Ptch1*$^{Wig/Wig}$ mutants still produce the 83kDa repressor form of Gli3, albeit at much reduced levels relative to wild type littermates. Furthermore, Ptch1^{Wig} protein is stable (Kurosaka et al., 2015), but cannot localize to the monocilium upon Smo stimulation in MDCK cells. Instead Ptch1^{Wig} localizes throughout the cytoplasm and cell surface. While we have no evidence that Ptch1^{Wig} can bind Shh, the ligand-binding region of Ptch1^{Wig} protein is intact. Thus, it is possible that Ptch1^{Wig} can inhibit Shh signaling by squelching Shh complexes with co-receptors, although proof of this mechanism requires further studies. Also that fact that Ptch1^{Wig} was unable to localize to monocilia upon Smo activation with small lipids, suggests that endocytosis of Ptch1 and Smo in response to Shh binding is abrogated in the *Ptch1*$^{Wig/Wig}$ mutants (Incardona et al., 2002). While previous

work has shown that activated Smo can localize to the monocilia of MDCK cells (Corbit et al., 2005), and we now report the localization of a direct Shh target (Ptch1) to the monocilium in response to the application of Smo agonists, it remains unknown if this results in pathway activation *via* the Gli proteins. It is therefore possible that localization of Ptch1 and Smo proteins in the monocilia of MDCK cells does not correlate with Shh pathway activation. To address the role of $Ptch1^{Wig}$ allele in directly regulating Shh signaling we focused on its effect on dorsal-ventral patterning of the embryonic spinal cord.

Genetically, the $Ptch1^{Wig}$ allele behaves as a *Shh* gain-of-function mutation. At E9.5, $Ptch1^{Wig/Wig}$ mutants displayed expansion of both p3 and floorplate progenitor identities, which normally overlap in the ventral-most region of the developing neural tube at this stage. This is consistent with previous observations showing that cells exposed to the highest concentration of Shh transiently express a gene regulatory network associated with cell fates elicited by the full range of Shh (Balaskas et al., 2012). Reciprocal genetic inhibitory loops then act to refine progenitor boundaries over time, which emerge as distinct domains of progenitor cells exposed to different levels of Shh signaling (Dessaud et al., 2007; Ribes and Briscoe, 2009; Briscoe and Small, 2015). In the case of the $Ptch1^{Wig/Wig}$ mutants, which exhibit decreased Gli3-repressor formation, and thus decreased inhibitory control of the Shh pathways, there is a greater transient response to the activation of ventral progenitor programs, which still resolve cell fates into discrete domains, albeit expanded and shifted dorsally. Thus, distinct progenitor domains still form in the $Ptch1^{Wig/Wig}$ mutants, which contrasts with *Ptch1* null mutants, that display a near complete conversion of neural fate to floorplate identity (Goodrich et al., 1997). This suggests that the $Ptch1^{Wig}$ mutation sensitizes the embryo to Shh signaling. Therefore we created $Hhat^{Creface/Creface};Ptch1^{Wig/Wig}$ compound mutants to test the idea that normal patterning can ensue in the $Ptch1^{Wig/Wig}$ mutant background provided that the levels of Shh are reduced. In this manner, the prolonged the exposure of cells to active Shh signaling in the $Ptch1^{Wig/Wig}$ mutants may be compensated by a diminished gradient in the *Hhat* mutants.

We previously reported that $Hhat^{Creface/Creface}$ mutants completely lack Shh activity (Dennis et al., 2012). This is supported by immunostaining for Shh protein levels suing the 5E1 antibody, which showed a lack of floorplate Shh staining in the $Hhat^{Creface/Creface};Ptch1^{Wig/Wig}$ compound mutants, despite robust mRNA expression. It is possible that Shh protein is mis-folded in the Hhat mutants and thus could not be detected by 5E1 antibody (Fuse et al., 1999). However, there is no evidence that *Hhat* loss impacts Shh folding and we did observe 5E1 immunostaining in the notochord of $Hhat^{Creface/Creface};Ptch1^{Wig/Wig}$ double mutants, suggesting Shh protein was folded correctly. The $Hhat^{Creface}$ mutation is therefore useful in addressing the role of the Shh activity gradient during neural patterning, as it greatly diminishes long range secretion of Shh from the floorplate, but does not completely abrogate Shh signaling (Dennis et al., 2012; Kurosaka et al., 2014; Kurosaka et al., 2015). Specifically, Hhat modifies the secreted form of Shh (*Shh-Np*) with a palmitoyate moiety that is essential to establish long range Shh signaling, thereby helping to create the Shh gradient (Pepinsky et al., 1998; Chamoun et al., 2001; Zeng et al., 2001; Dennis et al., 2012). $Hhat^{Creface/Creface}$ mutants exhibit Shh expression in the notochord, but not in the ventral neural tube. As a consequence, $Hhat^{Creface/Creface}$ mutants lack floorplate

and proper ventral spinal cord patterning, demonstrating that *Hhat* mutants lack the ability to generate secreted long-range Shh midline tissues.

We previously reported that $Hhat^{Creface/Creface}$; $Ptch1^{Wig/Wig}$ mutants rescued most of the mid-facial fusion and neurogenic placode defects in $Ptch1^{Wig/Wig}$ mutants, suggesting that the diminished repression of the Shh pathway in $Ptch1^{Wig/Wig}$ was counterbalanced by the loss of long range signaling form of Shh in the $Hhat^{Creface/Creface}$ mutants (Kurosaka et al., 2014; Kurosaka et al., 2015). Consistent with this idea, we now report that $Hhat^{Creface/Creface}$;$Ptch1^{Wig/Wig}$ double mutants exhibit full restoration of ventral spinal cord patterning, complete with the proper specification of floorplate, p3, and pMN progenitors. Despite an absence of Shh protein production from the floorplate, the size of the ventral domains was largely restored, thereby rescuing the enlarged and dorsally displaced p3 and pMN domains observed in $Ptch1^{Wig/Wig}$ mutants. These cell types require the highest levels of Shh signaling, yet in the $Hhat^{Creface/Creface}$;$Ptch1^{Wig/Wig}$ they developed normally, indicating that patterning can arise in embryos lacking long range Shh signaling. This study therefore highlights the complex nature of morphogen activity and suggests that neural patterning does not arise from a strict interpretation of a Shh concentration landscape. Instead our findings support the idea that patterning arises from the interplay between Shh signaling levels combined with modulation of repression to alter the responsiveness to Shh in target cells (Dessaud et al., 2007; Uygur et al., 2016).

Implications for the Shh morphogen gradient model

What is the implication for these findings for the Shh morphogen gradient model? First, our data supports a requirement for Shh signaling in cell fate specification in the ventral neural tube. Moreover, we show that Shh signaling from the notochord is necessary and sufficient to induce ventral patterning, since $Shh^{-/-}$; $Ptch1^{Wig/Wig}$ embryos, which lack Shh in the notochord and floorplate, exhibit only partially rescued neural patterning. In fact the ventral most cell types that require the highest levels of Shh, namely the floorplate and p3 interneurons, were not rescued in these double mutants. Secondly, our data implies that a Shh gradient principally acts in the ventral neural tube to overcome Ptch1-mediated inhibition of the pathway. Thus absolute levels of Shh or Gli activity are not sufficient to specify neural progenitor populations, but rather it is the relative balance of Gli activator and repressor that is crucial to setting up of distinct classes of neural cell fates, as has been argued previously (Junker et al., 2014; Uygur et al., 2016). This idea is also supported by previous work which showed that abnormal patterning of ventral cell identities in *Shh* mutants can be partially restored in $Shh^{-/-}$;$Gli3^{-/-}$ double mutants, and in $Ptch1^{-/-}$;$Gli2^{+/-}$;$Gli3^{-/-}$ combinatorial mutants (Litingtung and Chiang, 2000; Persson et al., 2002; Motoyama et al., 2003). Indeed the $Shh^{-/-}$;$Gli3^{-/-}$ largely resembled $Shh^{-/-}$; $Ptch1^{Wig/Wig}$ mutants, which is consistent with the function of Ptch1 in inhibiting activation of the Shh pathway (Junker et al., 2014). Our findings support the previous observation that Shh signaling in the floorplate is not essential for the initiation of patterning in the embryonic spinal cord (Yu et al., 2013). The initiation of neural patterning occurs during early embryogenesis when the notochord is in contact with the ventral midline of the developing neural tube (Tian et al., 2005; Chamberlain et al., 2008). Subsequently, continued Shh

signaling is required to stabilize ventral pattering and specify more dorsal classes of interneurons (Dessaud et al., 2010).

Conclusions

A morphogen is defined as a molecule secreted from a localized source that directs the differential acquisition of cell fates in naïve tissue as a function of the distance from the source (Balaskas et al., 2012; Briscoe and Small, 2015). That cells become patterned in response to a specific concentration of a secreted molecule is a central principal in developmental biology, and well supported, particularly by data generated in invertebrates (Nahmad and Stathopoulos, 2009; Swarup and Verheyen, 2012). Yet, in contrast to invertebrates, dissecting the complex genetics of morphogen gradients in vertebrate model systems is a challenge, thus the mechanistic regulation of Shh gradients remains incompletely understood (Briscoe and Small, 2015). Here we took advantage of mouse genetic models to alter the levels and distribution of Shh in the developing neural tube, and the responsiveness of target cells to Shh signaling by reducing a negative regulator of the pathway. We tested whether ventral spinal cord patterning could proceed normally in embryos lacking Shh secreted from the floorplate as well as missing a fully functional Ptch1 receptor. We conclude that the dynamic activation of neural progenitor regulatory networks remains very much intact in *Hhat*$^{Creface/Creface}$; *Ptch1*$^{Wig/Wig}$ mutants, demonstrating that ventral neural patterning can occur normally despite a severe reduction in the Shh activity gradient. Specifically, we showed that the enhanced responsiveness to Shh signaling in *Ptch1*$^{Wig/Wig}$ mutants could still be moderated during development such that by E10.5 the *Hhat*$^{Creface/Creface}$; *Ptch1*$^{Wig/Wig}$ neural tube is patterned normally, with floorplate, p3 and pMN progenitor domains forming sharp mutually exclusive boundaries at the appropriate dorsal-ventral limits. Implicit in the standard Shh morphogen model is the direct relationship between the concentration of Shh and the acquisition of specific cell types along the dorsal-ventral axis of the neural tube (Stamataki et al., 2005; Ribes and Briscoe, 2009; Dessaud et al., 2010; Balaskas et al., 2012; Junker et al., 2014; Briscoe and Small, 2015; Cohen et al., 2015). However, the diminished Shh activity gradient in *Hhat*$^{Creface/Creface}$ embryos can be compensated by the loss of pathway repression mediated by Ptch1, allowing for the sustained activation of downstream target genes, in a manner consistent with the a temporal adaptation mechanism (Dessaud et al., 2007; Dessaud et al., 2010). Our findings support the view that the precise regulation of both morphogen levels and the modulation of intrinsic responsiveness of target cells are required for neural patterning in the vertebrate embryo.

Experimental Procedures

Mice

The *Hhat*$^{Creface/Creface}$ and *Ptch1*$^{Wiggable/Wiggable}$ (*Ptch1*$^{Wig/Wig}$) mice were maintained as previously described (Sandell et al., 2011; Kurosaka et al., 2014; Kurosaka et al., 2015). *Hhat*$^{Creface/Creface}$ is an insertional mutation resulting in a null allele of the mouse Hedgehog aceyltransferase gene (Dennis et al., 2012). *Ptch1*$^{Wig/Wig}$ is an ENU-induced point mutation in intron 15 that crates a novel splice acceptor site, resulting in premature truncation of the Ptch1 protein in the region that encodes the 5th extracellular loop, as described previously

(Sandell et al., 2011; Kurosaka et al., 2015). *Ptch1*$^{Wig/Wig}$ mutants are viable until E11.5–12.5, while *Hhat*$^{Creface/Creface}$ mutants are viable until E16.5, allowing for an assessment of neural patterning in the spinal cord. A minimum of 5 embryos for each single mutant and 3–5 *Hhat*$^{Creface/Creface}$; *Ptch1*$^{Wig/Wig}$ double mutants were used for all immunohistochemistry experiments. *Ptch1*$^{LacZ/+}$ and *Shh*$^{+/-}$ (both are null alleles) mice were provided by the Jackson Laboratory and Dr Phil Beachy (Johns Hopkins University) respectively, and were maintained and genotyped as described previously (Kurosaka et al., 2015).

Preparation of Embryos for Immunohistochemistry, In Situ Hybridization, and β-galactosidase staining

E9.5–11.5 mouse embryos were obtained via timed mating, with the morning of detection of a vaginal plug being designated embryonic day (E)0.5. Embryos were collected at the desired stages in PBS, the extra embryonic tissues were removed, after which they were fixed for 1–2 hours in 4%PFA/PBS. The embryos were then cryoprotected by equilibrating in 15% sucrose/PBS and 30% sucrose/PBS, embedded in OCT (Tissue Tek) and sectioned on a cryostat at 12–14μm in a transverse plane. The following antibodies were used to assess dorsal-ventral pattering in the mouse neural tube: guinea pig anti-Olig2 (kind gift from Dr. Ben Novitch, UCLA, 1/5000), rabbit anti-Pax2 (Zymed, San Francisco, CA), mouse anti-Lim1/Lhx1 (DSHB, 4F2, 1/50); mouse anti-Sonic hedgehog (DSHB, 5E1, 1/40), mouse anti-Isl1/2 (DSHB, 39.4D5, 1/50), mouse anti-Nkx2.2 (74.5A5, 1/50), mouse anti-FoxA2 (4D7, 1/50), rabbit anti-FoxA2 (Abcam, 1/250), mouse anti-Pax3 (DSHB, 1/50), and mouse Pax6 (DSHB, 1/25). All mouse monoclonal antibodies were obtained from the Developmental Studies Hybridoma Bank (DSHB) developed under the auspices of the NICHD and maintained by the University of Iowa, Department of Biological Sciences (Iowa City, IA 52242). Species-specific Alexa Fluor 594 or 488-conjugated secondary antibodies were used at 1/1000 (Invitrogen, Carlsbad, CA). Sections were counterstained with DAPI (Sigma) prior to mounting with Dako fluorescent mounting medium (DakoCytomation, Carpinteria, CA). Whole-mount *in situ* hybridization using a *Shh* riboprobe and subsequent sectioning of stained embryos were performed as previously described (Kurosaka et al., 2014). Whole mount β-galactosidase (LacZ) staining and sectioning of *Ptch1*$^{LacZ/Wig}$ embryos were performed as previously described using a β-galactosidase staining kit (EMD-Millipore, Billerica, MA) (Kurosaka et al., 2015). All staining and statistical analyses were conducted on forelimb-level transverse sections of the embryonic spinal cord. Imaging was performing using a Zeiss Axiovert 200M microscope with 10X and 20X objectives or Zeiss AxioObserver with 20X objective and Apotome 2 structural illumination module, and processed using Photoshop CS6 (Adobe, San Jose, CA).

Statistical analysis of ventral patterning

For FoxA2 and Nkx2.2 immunostaining at E9.5, total cell counts were obtained from multiple 12μm forelimb bud level spinal cord sections of a minimum of N=3 wild type and *Ptch1*$^{Wig/Wig}$ mutant embryos. Statistical differences were calculated using a Student's t-test (Prism software) with the significance level set a $P<0.05$. Error bars reflect variance.

Ciliary localization studies

Mardin-Darby canine kidney II (MDCK II) cells were cultured in DMEM containing 10% fetal bovine serum (FBS) and Penicillin-Streptomycin-Fungizone at 37°C in a humidified incubator with 5% CO_2. Wild type Myc-Ptch1 and Flag-Ptch1^{Wig} cDNA constructs were cloned in pcDNA3.1 and transfected into MDCK II cells using Lipofectamine 2000 (Invitrogen) as previously described (Kurosaka et al., 2015). After 24 hours of transfection, cells were fixed for immunofluorescence staining. Transfected cells were briefly fixed with 4% paraformaldehyde (PFA) and permeabilized with a short wash in 0.5% TritonX-100. After blocking with 3% bovine serum albumin (BSA) in TBST (TBS + 0.1% Tween-20), cells were incubated overnight with antibodies to Flag-tag (Flag M2, Sigma, dilution 1/1000), c-Myc (9E10, Santa Cruz, dilution 1/500) and acetylated-tubulin (6-11B-1, Sigma, dilution 1/2000). Cells were washed with TBST, and incubated with appropriate secondary antibodies conjugated with Alexa Fluor 488 or 546 (Invitrogen) for 1 hour at room temperature. Nuclei were stained with DAPI. Fluorescence microscopy was performed on a Zeiss LSM5 PASCAL confocal microscope using a 63X objective. Confocal optical slices were collected and maximum-intensity projections of 0.2μm stacks were made using Zeiss LSM5 software.

Gli3 Western blots and quantification

To measure the formation of Gli3-repressor protein, Western blot analysis was performed using lysates from E10.5 wild type and *Ptch1*$^{Wig/Wig}$ mutant embryos. Whole embryos were lysed using RIPA lysis buffer with protease inhibitors and DTT, and resolved on a SDS-PAGE gel. Once transferred to nitrocellulose membranes, blots were blocked in 5% skim milk, followed by overnight incubation at 4°C using a Gli3 polyclonal antibody (a kind gift from Dr. Baolin Wang, Cornell Medical School, 1/200), and an α-tubulin antibody (Sigma, 1/5000) to control for loading. The following day, primary antibodies were remove, blots were rinsed in PBS + 0.1% Triton X100, and then re-incubated with Horseradish Peroxidase (HRP)-coupled secondary antibodies (Amersham, 1/500–1/1000). Blots were incubated with the Pierce Pico detection kit (ThermoFisher) according to manufacturer's recommendations and exposed to light-sensitive film. For quantification of Gli3 190/83 KDa ratios, 3 separate *Ptch1*$^{Wig/Wig}$ mutants and wild type littermates were used. Gli3 band intensity was quantified using ImageJ and normalized to β-actin. Statistical differences were calculated as above.

Acknowledgments

Funding

We would like to than the following agencies for funding support to AI: Natural Sciences and Engineering Council of Canada (RGPIN-2015-04475) and the Plum Foundation. Research in the Trainor lab is supported by Stowers Institute for Medical Research and the National Institutes of Dental and Craniofacial Research (DE016082).

We would like to thank Emily Capaldo (A.I. lab) for assistance with histology, Dr. Ben Novitch (UCLA) for the kind gift of Olig2 antibodies, and Dr. Baolin Wang (Cornell Medical School) for the kind gift of Gli3 antibodies. We also are grateful to the University of Iowa, Department of Biological Sciences (Iowa City, IA 52242) for maintaining the Developmental Studies Hybridoma Bank developed under the auspices of the NICHD that supplied much of the antibodies we used in this study. *Shh*$^{+/-}$ mice were generously provided by Dr Phil Beachy (Johns Hopkins University) and *Ptch1*$^{LacZ/+}$ mice were obtained from the Jackson Laboratory.

References

Agren M, Kogerman P, Kleman MI, Wessling M, Toftgard R. Expression of the PTCH1 tumor suppressor gene is regulated by alternative promoters and a single functional Gli-binding site. Gene. 2004; 330:101–114. [PubMed: 15087129]

Bai CB, Stephen D, Joyner AL. All mouse ventral spinal cord patterning by hedgehog is Gli dependent and involves an activator function of Gli3. Dev Cell. 2004; 6:103–115. [PubMed: 14723851]

Balaskas N, Ribeiro A, Panovska J, Dessaud E, Sasai N, Page KM, Briscoe J, Ribes V. Gene regulatory logic for reading the Sonic Hedgehog signaling gradient in the vertebrate neural tube. Cell. 2012; 148:273–284. [PubMed: 22265416]

Bangs F, Anderson KV. Primary Cilia and Mammalian Hedgehog Signaling. Cold Spring Harb Perspect Biol. 2016

Briscoe J, Pierani A, Jessell TM, Ericson J. A homeodomain protein code specifies progenitor cell identity and neuronal fate in the ventral neural tube. Cell. 2000; 101:435–445. [PubMed: 10830170]

Briscoe J, Small S. Morphogen rules: design principles of gradient-mediated embryo patterning. Development. 2015; 142:3996–4009. [PubMed: 26628090]

Caspary T, Larkins CE, Anderson KV. The graded response to Sonic Hedgehog depends on cilia architecture. Dev Cell. 2007; 12:767–778. [PubMed: 17488627]

Chamberlain CE, Jeong J, Guo C, Allen BL, McMahon AP. Notochord-derived Shh concentrates in close association with the apically positioned basal body in neural target cells and forms a dynamic gradient during neural patterning. Development. 2008; 135:1097–1106. [PubMed: 18272593]

Chamoun Z, Mann RK, Nellen D, von Kessler DP, Bellotto M, Beachy PA, Basler K. Skinny hedgehog, an acyltransferase required for palmitoylation and activity of the hedgehog signal. Science. 2001; 293:2080–2084. [PubMed: 11486055]

Chen Y, Struhl G. Dual roles for patched in sequestering and transducing Hedgehog. Cell. 1996; 87:553–563. [PubMed: 8898207]

Cohen M, Kicheva A, Ribeiro A, Blassberg R, Page KM, Barnes CP, Briscoe J. Ptch1 and Gli regulate Shh signalling dynamics via multiple mechanisms. Nat Commun. 2015; 6:6709. [PubMed: 25833741]

Corbit KC, Aanstad P, Singla V, Norman AR, Stainier DY, Reiter JF. Vertebrate Smoothened functions at the primary cilium. Nature. 2005; 437:1018–1021. [PubMed: 16136078]

Cortellino S, Wang C, Wang B, Bassi MR, Caretti E, Champeval D, Calmont A, Jarnik M, Burch J, Zaret KS, Larue L, Bellacosa A. Defective ciliogenesis, embryonic lethality and severe impairment of the Sonic Hedgehog pathway caused by inactivation of the mouse complex A intraflagellar transport gene Ift122/Wdr10, partially overlapping with the DNA repair gene Med1/Mbd4. Dev Biol. 2009; 325:225–237. [PubMed: 19000668]

Dennis JF, Kurosaka H, Iulianella A, Pace J, Thomas N, Beckham S, Williams T, Trainor PA. Mutations in Hedgehog acyltransferase (Hhat) perturb Hedgehog signaling, resulting in severe acrania-holoprosencephaly-agnathia craniofacial defects. PLoS Genet. 2012; 8:e1002927. [PubMed: 23055936]

Dessaud E, McMahon AP, Briscoe J. Pattern formation in the vertebrate neural tube: a sonic hedgehog morphogen-regulated transcriptional network. Development. 2008; 135:2489–2503. [PubMed: 18621990]

Dessaud E, Ribes V, Balaskas N, Yang LL, Pierani A, Kicheva A, Novitch BG, Briscoe J, Sasai N. Dynamic assignment and maintenance of positional identity in the ventral neural tube by the morphogen sonic hedgehog. PLoS Biol. 2010; 8:e1000382. [PubMed: 20532235]

Dessaud E, Yang LL, Hill K, Cox B, Ulloa F, Ribeiro A, Mynett A, Novitch BG, Briscoe J. Interpretation of the sonic hedgehog morphogen gradient by a temporal adaptation mechanism. Nature. 2007; 450:717–720. [PubMed: 18046410]

Drummond IA. Cilia functions in development. Curr Opin Cell Biol. 2012; 24:24–30. [PubMed: 22226236]

Echelard Y, Epstein DJ, St-Jacques B, Shen L, Mohler J, McMahon JA, McMahon AP. Sonic hedgehog, a member of a family of putative signaling molecules, is implicated in the regulation of CNS polarity. Cell. 1993; 75:1417–1430. [PubMed: 7916661]

Eggenschwiler JT, Anderson KV. Cilia and developmental signaling. Annu Rev Cell Dev Biol. 2007; 23:345–373. [PubMed: 17506691]

Ericson J, Briscoe J, Rashbass P, van Heyningen V, Jessell TM. Graded sonic hedgehog signaling and the specification of cell fate in the ventral neural tube. Cold Spring Harb Symp Quant Biol. 1997; 62:451–466. [PubMed: 9598380]

Ericson J, Muhr J, Placzek M, Lints T, Jessell TM, Edlund T. Sonic hedgehog induces the differentiation of ventral forebrain neurons: a common signal for ventral patterning within the neural tube. Cell. 1995; 81:747–756. [PubMed: 7774016]

Fuse N, Maiti T, Wang B, Porter JA, Hall TM, Leahy DJ, Beachy PA. Sonic hedgehog protein signals not as a hydrolytic enzyme but as an apparent ligand for patched. Proc Natl Acad Sci U S A. 1999; 96:10992–10999. [PubMed: 10500113]

Goodrich LV, Milenkovic L, Higgins KM, Scott MP. Altered neural cell fates and medulloblastoma in mouse patched mutants. Science. 1997; 277:1109–1113. [PubMed: 9262482]

He M, Agbu S, Anderson KV. Microtubule Motors Drive Hedgehog Signaling in Primary Cilia. Trends Cell Biol. 2017; 27:110–125. [PubMed: 27765513]

Huangfu D, Anderson KV. Cilia and Hedgehog responsiveness in the mouse. Proc Natl Acad Sci U S A. 2005; 102:11325–11330. [PubMed: 16061793]

Huangfu D, Anderson KV. Signaling from Smo to Ci/Gli: conservation and divergence of Hedgehog pathways from Drosophila to vertebrates. Development. 2006; 133:3–14. [PubMed: 16339192]

Huangfu D, Liu A, Rakeman AS, Murcia NS, Niswander L, Anderson KV. Hedgehog signalling in the mouse requires intraflagellar transport proteins. Nature. 2003; 426:83–87. [PubMed: 14603322]

Incardona JP, Gruenberg J, Roelink H. Sonic hedgehog induces the segregation of patched and smoothened in endosomes. Curr Biol. 2002; 12:983–995. [PubMed: 12123571]

Jacob J, Briscoe J. Gli proteins and the control of spinal-cord patterning. EMBO Rep. 2003; 4:761–765. [PubMed: 12897799]

Junker JP, Peterson KA, Nishi Y, Mao J, McMahon AP, van Oudenaarden A. A predictive model of bifunctional transcription factor signaling during embryonic tissue patterning. Dev Cell. 2014; 31:448–460. [PubMed: 25458012]

Kurosaka H, Iulianella A, Williams T, Trainor PA. Disrupting hedgehog and WNT signaling interactions promotes cleft lip pathogenesis. J Clin Invest. 2014; 124:1660–1671. [PubMed: 24590292]

Kurosaka H, Trainor PA, Leroux-Berger M, Iulianella A. Cranial nerve development requires co-ordinated Shh and canonical Wnt signaling. PLoS One. 2015; 10:e0120821. [PubMed: 25799573]

Larkins CE, Aviles GD, East MP, Kahn RA, Caspary T. Arl13b regulates ciliogenesis and the dynamic localization of Shh signaling proteins. Mol Biol Cell. 2011; 22:4694–4703. [PubMed: 21976698]

Lei Q, Zelman AK, Kuang E, Li S, Matise MP. Transduction of graded Hedgehog signaling by a combination of Gli2 and Gli3 activator functions in the developing spinal cord. Development. 2004; 131:3593–3604. [PubMed: 15215207]

Litingtung Y, Chiang C. Specification of ventral neuron types is mediated by an antagonistic interaction between Shh and Gli3. Nat Neurosci. 2000; 3:979–985. [PubMed: 11017169]

Liu A, Wang B, Niswander LA. Mouse intraflagellar transport proteins regulate both the activator and repressor functions of Gli transcription factors. Development. 2005; 132:3103–3111. [PubMed: 15930098]

Marigo V, Davey RA, Zuo Y, Cunningham JM, Tabin CJ. Biochemical evidence that patched is the Hedgehog receptor. Nature. 1996; 384:176–179. [PubMed: 8906794]

Matise MP. Molecular genetic control of cell patterning and fate determination in the developing ventral spinal cord. Wiley Interdiscip Rev Dev Biol. 2013; 2:419–425. [PubMed: 23799585]

McMahon AP, Hasso SM. Filopodia: the cellular quills of hedgehog signaling? Dev Cell. 2013; 25:328–330. [PubMed: 23725760]

Motoyama J, Milenkovic L, Iwama M, Shikata Y, Scott MP, Hui CC. Differential requirement for Gli2 and Gli3 in ventral neural cell fate specification. Dev Biol. 2003; 259:150–161. [PubMed: 12812795]

Murdoch JN, Copp AJ. The relationship between sonic Hedgehog signaling, cilia, and neural tube defects. Birth Defects Res A Clin Mol Teratol. 2010; 88:633–652. [PubMed: 20544799]

Nahmad M, Stathopoulos A. Dynamic interpretation of hedgehog signaling in the Drosophila wing disc. PLoS Biol. 2009; 7:e1000202. [PubMed: 19787036]

Oh S, Huang X, Liu J, Litingtung Y, Chiang C. Shh and Gli3 activities are required for timely generation of motor neuron progenitors. Dev Biol. 2009; 331:261–269. [PubMed: 19433083]

Pal K, Mukhopadhyay S. Primary cilium and sonic hedgehog signaling during neural tube patterning: role of GPCRs and second messengers. Dev Neurobiol. 2015; 75:337–348. [PubMed: 24863049]

Pepinsky RB, Zeng C, Wen D, Rayhorn P, Baker DP, Williams KP, Bixler SA, Ambrose CM, Garber EA, Miatkowski K, Taylor FR, Wang EA, Galdes A. Identification of a palmitic acid-modified form of human Sonic hedgehog. J Biol Chem. 1998; 273:14037–14045. [PubMed: 9593755]

Persson M, Stamataki D, te Welscher P, Andersson E, Bose J, Ruther U, Ericson J, Briscoe J. Dorsal-ventral patterning of the spinal cord requires Gli3 transcriptional repressor activity. Genes Dev. 2002; 16:2865–2878. [PubMed: 12435629]

Qin J, Lin Y, Norman RX, Ko HW, Eggenschwiler JT. Intraflagellar transport protein 122 antagonizes Sonic Hedgehog signaling and controls ciliary localization of pathway components. Proc Natl Acad Sci U S A. 2011; 108:1456–1461. [PubMed: 21209331]

Ribes V, Briscoe J. Establishing and interpreting graded Sonic Hedgehog signaling during vertebrate neural tube patterning: the role of negative feedback. Cold Spring Harb Perspect Biol. 2009; 1:a002014. [PubMed: 20066087]

Rohatgi R, Milenkovic L, Scott MP. Patched1 regulates hedgehog signaling at the primary cilium. Science. 2007; 317:372–376. [PubMed: 17641202]

Ruiz i Altaba A. Combinatorial Gli gene function in floor plate and neuronal inductions by Sonic hedgehog. Development. 1998; 125:2203–2212. [PubMed: 9584120]

Sandell LL, Iulianella A, Melton KR, Lynn M, Walker M, Inman KE, Bhatt S, Leroux-Berger M, Crawford M, Jones NC, Dennis JF, Trainor PA. A phenotype-driven ENU mutagenesis screen identifies novel alleles with functional roles in early mouse craniofacial development. genesis. 2011; 49:342–359. [PubMed: 21305688]

Sanders TA, Llagostera E, Barna M. Specialized filopodia direct long-range transport of SHH during vertebrate tissue patterning. Nature. 2013; 497:628–632. [PubMed: 23624372]

Sasaki H, Nishizaki Y, Hui C, Nakafuku M, Kondoh H. Regulation of Gli2 and Gli3 activities by an amino-terminal repression domain: implication of Gli2 and Gli3 as primary mediators of Shh signaling. Development. 1999; 126:3915–3924. [PubMed: 10433919]

Stamataki D, Ulloa F, Tsoni SV, Mynett A, Briscoe J. A gradient of Gli activity mediates graded Sonic Hedgehog signaling in the neural tube. Genes Dev. 2005; 19:626–641. [PubMed: 15741323]

Stone DM, Hynes M, Armanini M, Swanson TA, Gu Q, Johnson RL, Scott MP, Pennica D, Goddard A, Phillips H, Noll M, Hooper JE, de Sauvage F, Rosenthal A. The tumour-suppressor gene patched encodes a candidate receptor for Sonic hedgehog. Nature. 1996; 384:129–134. [PubMed: 8906787]

Swarup S, Verheyen EM. Wnt/Wingless signaling in Drosophila. Cold Spring Harb Perspect Biol. 2012:4.

Taipale J, Cooper MK, Maiti T, Beachy PA. Patched acts catalytically to suppress the activity of Smoothened. Nature. 2002; 418:892–897. [PubMed: 12192414]

Tian H, Jeong J, Harfe BD, Tabin CJ, McMahon AP. Mouse Disp1 is required in sonic hedgehog-expressing cells for paracrine activity of the cholesterol-modified ligand. Development. 2005; 132:133–142. [PubMed: 15576405]

Uygur A, Young J, Huycke TR, Koska M, Briscoe J, Tabin CJ. Scaling Pattern to Variations in Size during Development of the Vertebrate Neural Tube. Dev Cell. 2016; 37:127–135. [PubMed: 27093082]

Wang B, Fallon JF, Beachy PA. Hedgehog-regulated processing of Gli3 produces an anterior/posterior repressor gradient in the developing vertebrate limb. Cell. 2000; 100:423–434. [PubMed: 10693759]

Wang C, Ruther U, Wang B. The Shh-independent activator function of the full-length Gli3 protein and its role in vertebrate limb digit patterning. Dev Biol. 2007; 305:460–469. [PubMed: 17400206]

Xiong F, Tentner AR, Huang P, Gelas A, Mosaliganti KR, Souhait L, Rannou N, Swinburne IA, Obholzer ND, Cowgill PD, Schier AF, Megason SG. Specified neural progenitors sort to form sharp domains after noisy Shh signaling. Cell. 2013; 153:550–561. [PubMed: 23622240]

Yamada T, Pfaff SL, Edlund T, Jessell TM. Control of cell pattern in the neural tube: motor neuron induction by diffusible factors from notochord and floor plate. Cell. 1993; 73:673–686. [PubMed: 8500163]

Yamada T, Placzek M, Tanaka H, Dodd J, Jessell TM. Control of cell pattern in the developing nervous system: polarizing activity of the floor plate and notochord. Cell. 1991; 64:635–647. [PubMed: 1991324]

Yu K, McGlynn S, Matise MP. Floor plate-derived sonic hedgehog regulates glial and ependymal cell fates in the developing spinal cord. Development. 2013; 140:1594–1604. [PubMed: 23482494]

Zeng X, Goetz JA, Suber LM, Scott WJ Jr, Schreiner CM, Robbins DJ. A freely diffusible form of Sonic hedgehog mediates long-range signalling. Nature. 2001; 411:716–720. [PubMed: 11395778]

Zhang XM, Ramalho-Santos M, McMahon AP. Smoothened mutants reveal redundant roles for Shh and Ihh signaling including regulation of L/R symmetry by the mouse node. Cell. 2001; 106:781–792. [PubMed: 11517919]

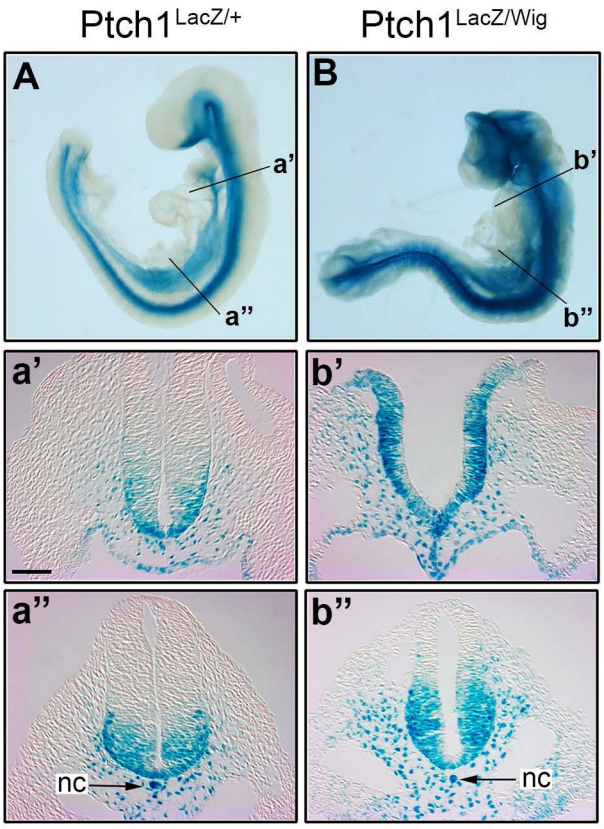

Figure 1.

Ptch1$^{Wig/Wig}$ mutants display expanded Shh signaling in the developing neural tube. (**A, B**). Whole mount β–galactosidase staining of E9.5 *Ptch1*$^{LacZ/+}$ heterozygotes (**A**) and *Ptch1*$^{LacZ/Wig}$ mutants (**B**) showing increased staining in the mutants. Transverse sections at two different axial levels (**a′, a″, b′, b″**) indicated in whole mount images, reveal extent of expanded LacZ activity in *Ptch1*$^{LacZ/Wig}$ mutants (**b′, b″**). Whole mount images in (**A, B**) modified from (Kurosaka et al., 2015). Scale, (a′) 50μm.

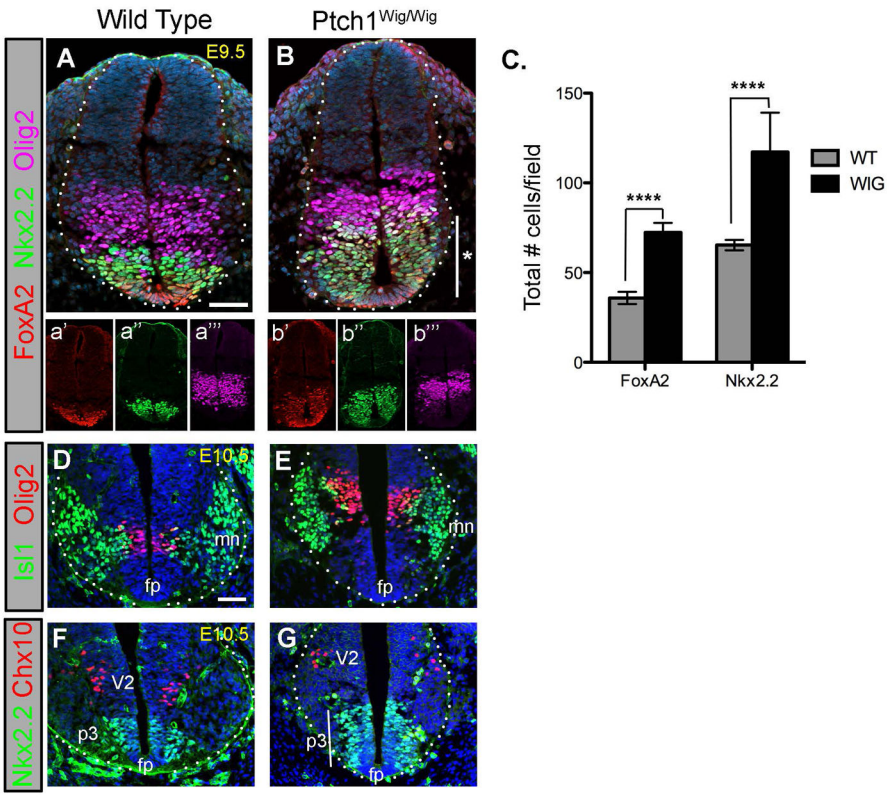

Figure 2.

Ptch1$^{Wig/Wig}$ mutants display expanded ventral neural patterning. (**A, B**) FoxA2 (red, a′, b′), Nkx2.2 (green, a″, b″), and Olig2 (magenta, a‴, b‴) co-staining of E9.5 wild type (**A-a‴**) and *Ptch1*$^{Wig/Wig}$ mutant (**B-b‴**) neural tubes showing expanded ventral progenitor domains in the mutant. There was a greater overlap of FoxA2 and Nkx2.2-positive cells in the *Ptch1*$^{Wig/Wig}$ mutants (**B**,* **). (C)** Quantification of significant increases in the numbers of FoxA2 and Nkx2.2 expressing progenitors in the *Ptch1*$^{Wig/Wig}$ mutants relative to wild type controls (****, P<0.0001). (**D, E**) Olig2 (red) and Isl1 (green) staining of E10.5 wild type (**D**) and *Ptch1*$^{Wig/Wig}$ mutant (**E**) neural tubes showing dorsal displacement and expansion of the MN domain. (**F, G**) Chx10 (red) and Nkx2.2 (green) staining of E10.5 wild type (**F**) and *Ptch1*$^{Wig/Wig}$ mutant (**G**) neural tubes showing p3 expansion (*) and dorsal displacement of Chx10-positive V2 interneurons in mutants. DAPI staining (blue) identifies nuclei. FP, floorplate; p3, V3 interneuron progenitors; pMN, motor neuron progenitors. Scale (A, D) 50μm.

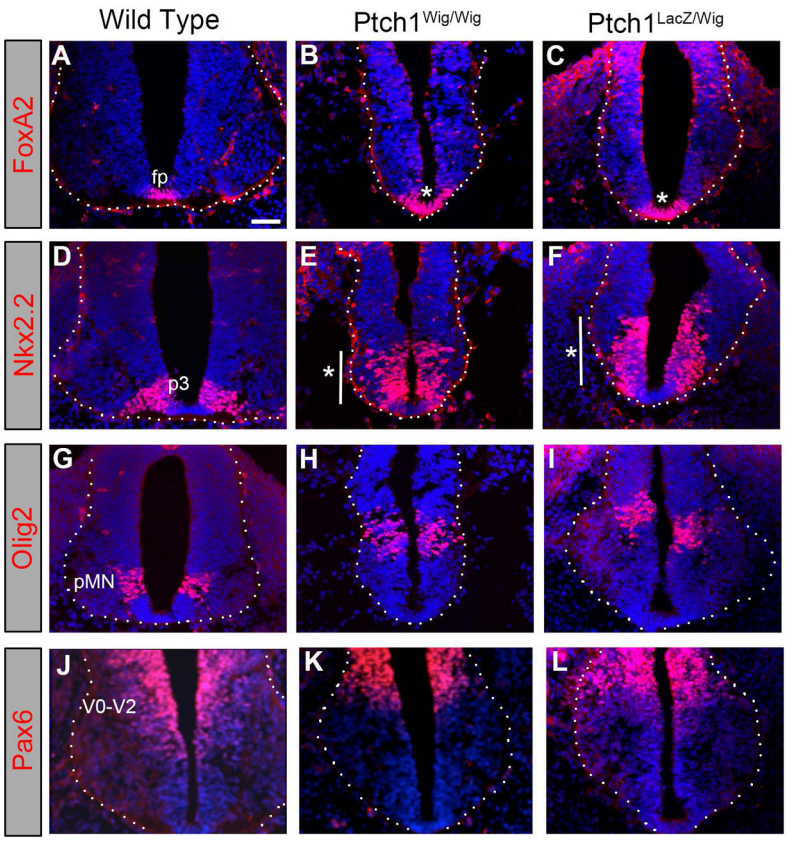

Figure 3.

Ptch1$^{Wig/Wig}$ and *Ptch1*$^{LacZ/Wig}$ embryos display similar expansions of ventral neural character. (**A–C**) FoxA2 staining of floorplate cells in E10.5 wild type (**A**), *Ptch1*$^{Wig/Wig}$ (**B**), and *Ptch1*$^{LacZ/Wig}$ (**C**), showing floorplate expansion (*). (**D–F**) Nkx2.2 staining in E10.5 wild type (**D**), *Ptch1*$^{Wig/Wig}$ (**E**), and *Ptch1*$^{LacZ/Wig}$ (**F**), showing expanded V3 interneuron progenitors (*). (**G–I**) Olig2 staining in E10.5 wild type (**G**), *Ptch1*$^{Wig/Wig}$ (**H**) and *Ptch1*$^{LacZ/Wig}$ (**I**) mutants, showing dorsally displaced motoneuron progenitors in both mutants. (**J–L**) Pax6 staining in E10.5 wild type (**D**), *Ptch1*$^{Wig/Wig}$ (**E**) and *Ptch1*$^{LacZ/Wig}$ (**F**) mutants, showing displaced interneuron progenitor domains in the mutants. DAPI staining (blue) identifies nuclei. Fp, floorplate; p3, V3 progenitors; pMN, motorneuron progenitors; V0-V2, ventral interneurons. Scale (A) 50μm.

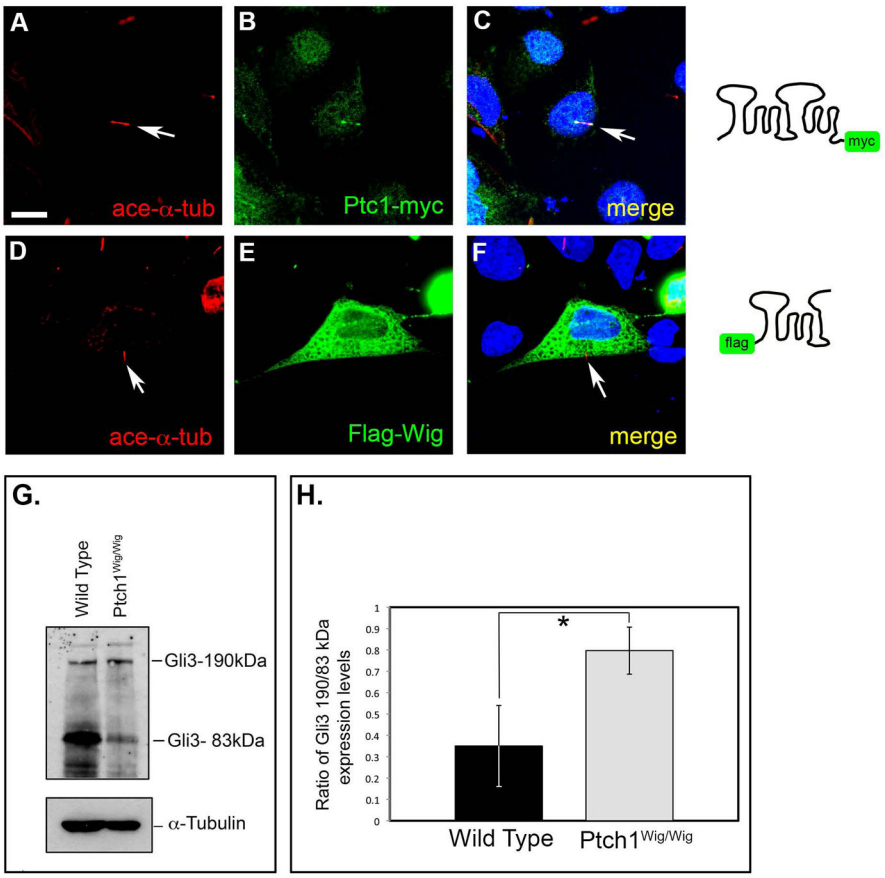

Figure 4.

Ptch1^{Wig} fails to localize to cilia and shows reduced Gli3-Repressor formation. (**A–F**) Immunofluorescence images of cells transfected with expression construct of C-terminal myc-tagged Ptch1 (Ptch1-myc; **A–C**) and N-terminal flag-tagged Ptch1^{Wig} (Flag-Wig; **D–F**). Schematic diagrams of Ptch1-myc and Flag-Wig (right side of panels) are shown. 20-hydroxycholesterol treated transfected cells were immunostained for acetylated-α-tubulin to label cilia (**A**, **D**). Sub-cellular localization of Ptch1-myc and Flag-Wig proteins were detected using antibodies recognizing Myc (**B**) and Flag (**E**) epitope tags, respectively. DAPI staining in blue identifies nuclei. Scale (A) 5μm. (**G**) Western blot of lysates from E11.5 wild type and *Ptch1$^{Wig/Wig}$* mutant embryos using Gli3 antibodies to detect full length (190kDa) and repressor (83kDa) forms, and α-tubulin as loading control. (**H**) Quantification of Gli3 full-length/repressor forms showing increased ratio in *Ptch1$^{Wig/Wig}$* mutants, reflecting decreased repressor synthesis.

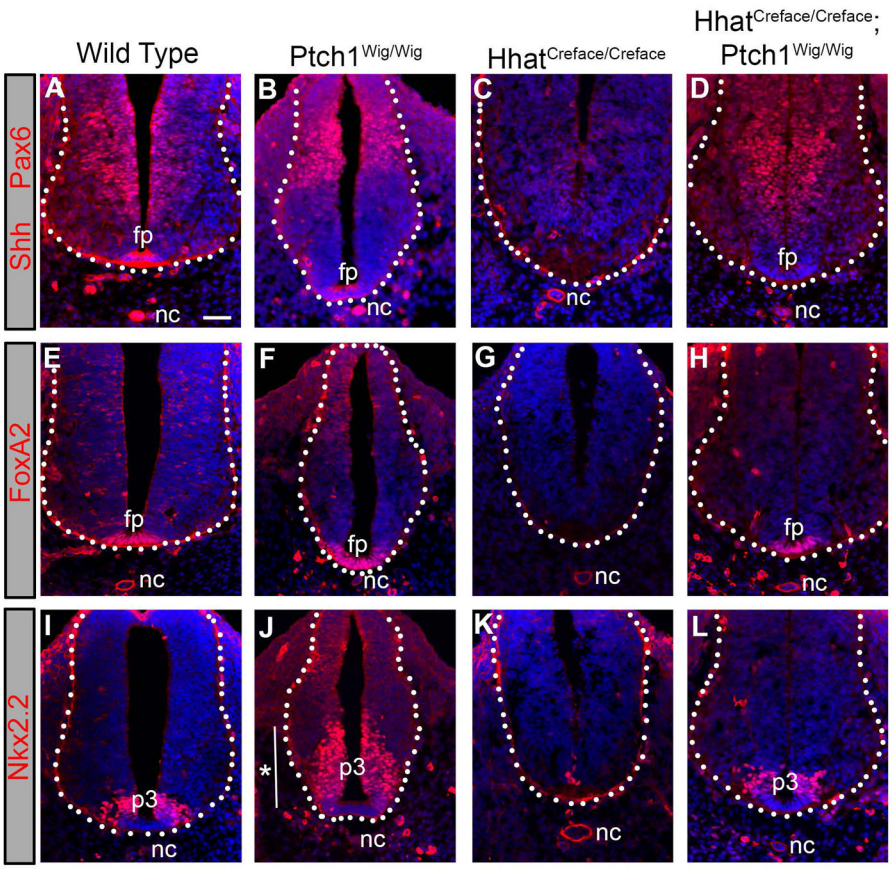

Figure 5.

Complete rescue of ventral neural patterning defects in *Hhat*$^{Creface/Creface}$*; Ptch1*$^{Wig/Wig}$ double mutants. (**A–D**) Combined Pax6 and Shh immunostaining in transverse neural tube sections of E10.5 wild type (**A**), *Ptch1*$^{Wig/Wig}$ (**B**) and *Hhat*$^{Creface/Creface}$ (**C**) single mutants, and *Hhat*$^{Creface/Creface}$*; Ptch1*$^{Wig/Wig}$ double mutant (**D**). *Hhat*$^{Creface/Creface}$*; Ptch1*$^{Wig/Wig}$ double mutant showed a restoration of ventral progenitor domain despite lacking Shh protein expression from the floorplate. (**E–H**) FoxA2 immunostaining in wild type (**E**), *Ptch1*$^{Wig/Wig}$ (**F**) and *Hhat*$^{Creface/Creface}$ (**G**) single mutants, and *Hhat*$^{Creface/Creface}$*; Ptch1*$^{Wig/Wig}$ double mutant (**H**). *Hhat*$^{Creface/Creface}$*; Ptch1*$^{Wig/Wig}$ double mutant showed a restoration of floorplate identity. (**I–L**) Nkx2.2 immunostaining identified V3 progenitors in wild type (**I**), *Ptch1*$^{Wig/Wig}$ (**J**) and *Hhat*$^{Creface/Creface}$ (**K**) single mutants, and *Hhat*$^{Creface/Creface}$*; Ptch1*$^{Wig/Wig}$ double mutant (**L**). (**J**) *Ptch1*$^{Wig/Wig}$ mutants displayed expanded V3 progenitors (*), in contrast *Hhat*$^{Creface/Creface}$ (**K**) showed a loss of V3 specification, while *Hhat*$^{Creface/Creface}$*; Ptch1*$^{Wig/Wig}$ double mutant (**L**) showed a restoration of the V3 progenitor domain. Fp, floorplate; p3, V3 progenitors; nc, notochord. Scale (A) 50μm.

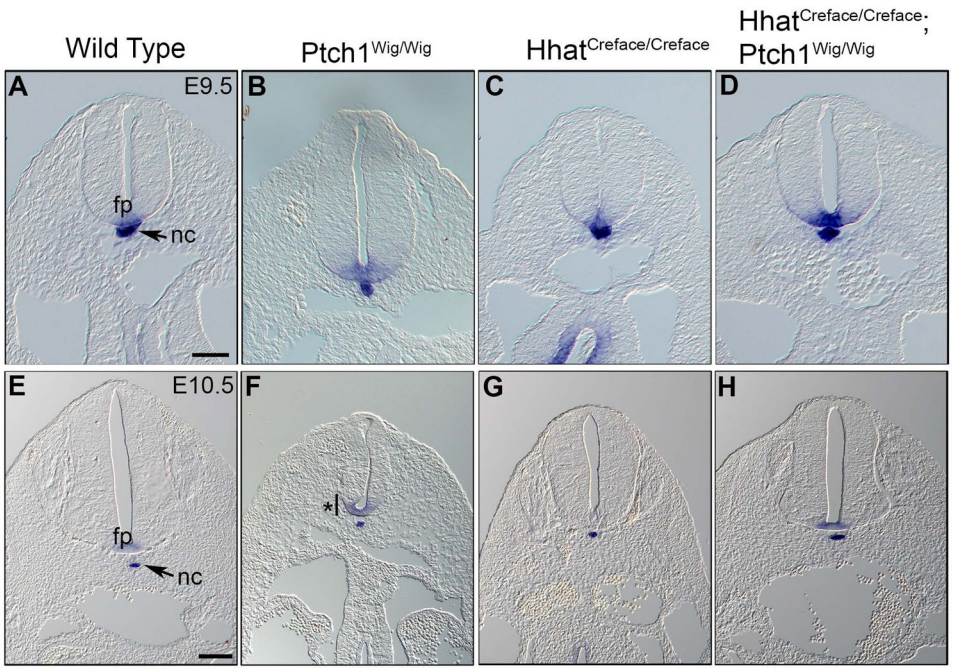

Figure 6.

Rescued floorplate specification in *Hhat*$^{Creface/Creface}$*; Ptch1*$^{Wig/Wig}$ double mutants. *Shh in situ* hybridization (ISH) revealing floorplate specification in *Ptch1*$^{Wig/Wig}$ and *Hhat*$^{Creface/Creface}$ single and double mutants. *Shh* ISH of spinal cord sections at E9.5 (**A–D**) and E10.5 (**E–H**) for wild type (**A, E**), *Ptch1*$^{Wig/Wig}$ (**B, F**), *Hhat*$^{Creface/Creface}$ (**C, G**), and *Hhat*$^{Creface/Creface}$*; Ptch1*$^{Wig/Wig}$ (**D, H**) embryos. Scale (A) 50μm, (E) 100μm.

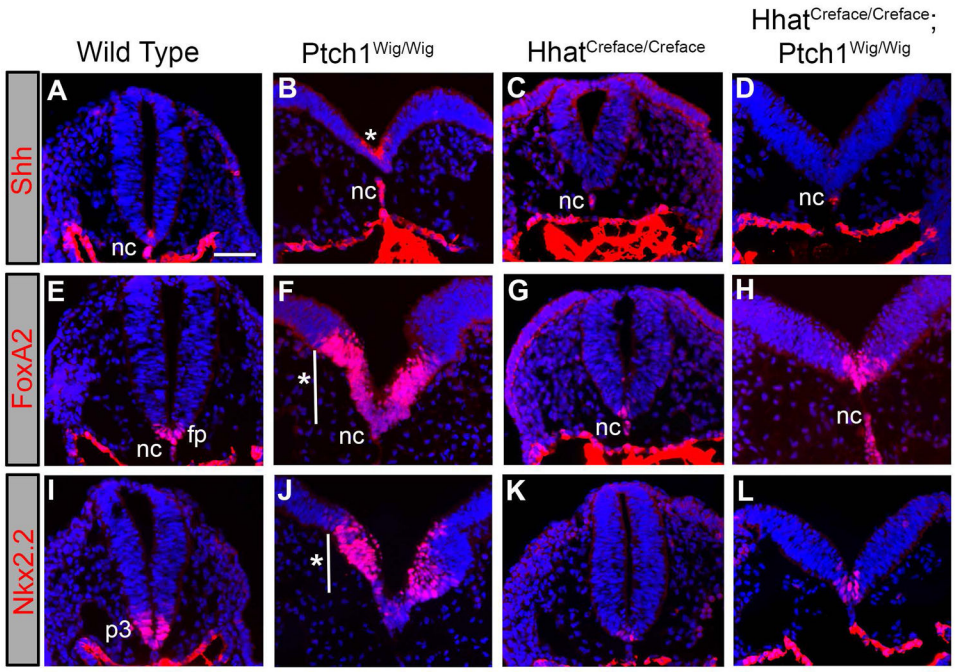

Figure 7.

Hhat$^{Creface/Creface}$*; Ptch1*$^{Wig/Wig}$ double mutants show incomplete restoration of ventral progenitor domains in the early embryonic neural tube. (**A–D**) Shh immunostaining in E8.5 neural tubes of wild type (**A**), *Ptch1*$^{Wig/Wig}$ (**B**) and *Hhat*$^{Creface/Creface}$ (**C**) single mutants, and *Hhat*$^{Creface/Creface}$*; Ptch1*$^{Wig/Wig}$ double mutant (**D**). The *Ptch1*$^{Wig/Wig}$ mutant showed an expanded Shh expression in the ventral neural tube (*, **B**), while the *Hhat*$^{Creface/Creface}$ (**C**) and *Hhat*$^{Creface/Creface}$*; Ptch1*$^{Wig/Wig}$ double mutant (**D**) lacked Shh expression in the ventral neural tube, but mainateained Shh in the notochord. (**E–F**) FoxA2 immunostaining in wild type (**E**), *Ptch1*$^{Wig/Wig}$ (**F**) and *Hhat*$^{Creface/Creface}$ (**G**) single mutants, and *Hhat*$^{Creface/Creface}$*; Ptch1*$^{Wig/Wig}$ double mutant (**H**). The *Ptch1*$^{Wig/Wig}$ mutant displayed an expanded floorplate domain (*, **F**), while the *Hhat*$^{Creface/Creface}$ mutant showed greatly reduced floorplate specification (**G**), and the *Hhat*$^{Creface/Creface}$*; Ptch1*$^{Wig/Wig}$ double mutant (H) displayed an intermediate level of floorplate expansion (**H**). (**I–L**) Nkx2.2 immunostaining in E8.5 neural tubes of wild type (**I**), *Ptch1*$^{Wig/Wig}$ (**J**) and *Hhat*$^{Creface/Creface}$ (**K**) single mutants, and *Hhat*$^{Creface/Creface}$*; Ptch1*$^{Wig/Wig}$ double mutant (**L**). The *Ptch1*$^{Wig/Wig}$ mutant showed expanded p3 domain (*, **J**), while the *Hhat*$^{Creface/Creface}$ mutant showed diminished floorplate specification (**K**), which was restored to near wild type levels in the *Hhat*$^{Creface/Creface}$*; Ptch1*$^{Wig/Wig}$ double mutant (**L**). Fp, floorplate; p3, V3 progenitors; nc, notochord. Scale (A) 50μm.

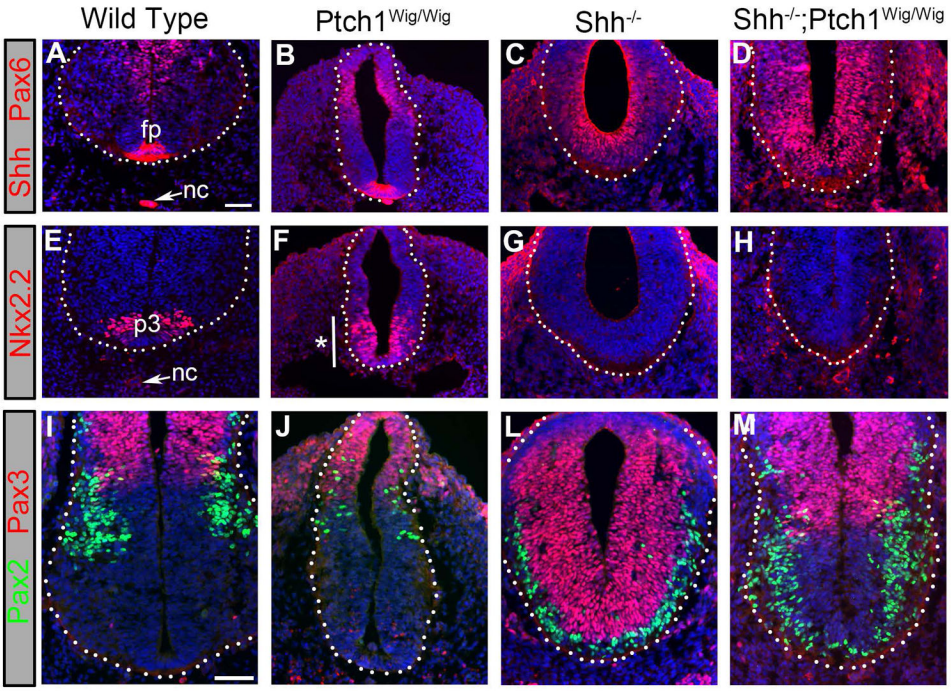

Figure 8.

Partial rescue of ventral patterning in *Shh*$^{-/-}$*;Ptch1*$^{Wig/Wig}$ mutants. (**A–D**) Combined Pax6 and Shh immunostaining in transverse neural tube sections of E10.5 wild type (**A**), *Ptch1*$^{Wig/Wig}$ (**B**) and *Shh*$^{-/-}$ (**C**) single mutants, and *Shh*$^{-/-}$*; Ptch1*$^{Wig/Wig}$ double mutant (**D**). (**C**) Shh$^{-/-}$ mutants lack ventral specification and did not develop a floorplate. (**D**) *Shh*$^{-/-}$*; Ptch1*$^{Wig/Wig}$ double mutants showed expanded Pax6-positve ventral interneurons throughout the neural tube and lacked a floorplate. (**E–H**) Nkx2.2 staining of wild type (**E**), *Ptch1*$^{Wig/Wig}$ (**F**) and *Shh*$^{-/-}$ (**G**) single mutants, and *Shh*$^{-/-}$*; Ptch1*$^{Wig/Wig}$ double mutant (**H**). Expanded p3 domain in *Ptch1*$^{Wig/Wig}$ mutants (*, F), in contrast to *Shh*$^{-/-}$ *single (G) and Shh*$^{-/-}$*; Ptch1*$^{Wig/Wig}$ double (H) mutants, which lack p3 formation. (I–M) Pax2 (green) and Pax3 (red) immunostaining for interneurons in wild type (**I**), *Ptch1*$^{Wig/Wig}$ (**J**) and *Shh*$^{-/-}$ (**L**) single mutants, and *Shh*$^{-/-}$*; Ptch1*$^{Wig/Wig}$ double mutant (**M**). Pax2 labels medial interneuron groups, while Pax3 labels dorsal interneurons progenitors. (**J**) *Ptch1*$^{Wig/Wig}$ mutants displayed dorsally shifted Pax2-positive cells and reduced Pax3-positive projectors. (**L**) Shh$^{-/-}$ mutant displayed dorsalized neural tubes with both Pax2 (green) and Pax3 (red) positive cells expanded throughout the ventral neural tube, which lacked a floorplate. (**M**) Partial rescue of the Pax3 dorsal domain boundary in *Shh*$^{-/-}$*; Ptch1*$^{Wig/Wig}$ double mutants, while Pax2-positve interneurons remained expanded throughout the ventral neural tube, which lacked a floorplate. Scale (A, I) 50μm.